A synthetic semi-empirical physical model of secondary electron yield of metals under E-beam irradiation*

Guo-Bao Feng(封国宝)[1,2], Wan-Zhao Cui(崔万照)[1,†], Na Zhang(张娜)[1], Meng Cao(曹猛)[2], and Chun-Liang Liu(刘纯亮)[2]

[1] National Key Laboratory of Science and Technology on Space Microwave, Xi'an 710000, China
[2] Key Laboratory for Physical Electronics and Devices of the Ministry of Education, Department of Electronic Science and Technology, Xi'an Jiaotong University, Xi'an 710049, China

(Received 7 April 2017; revised manuscript received 24 May 2017; published online 1 August 2017)

Calculations of secondary electron yield (SEY) by physical formula can hardly accord with experimental results precisely. Simplified descriptions of internal electron movements in the calculation and complex surface contamination states of real sample result in notable difference between simulations and experiments. In this paper, in order to calculate SEY of metal under complicated surface state accurately, we propose a synthetic semi-empirical physical model. The processes of excitation of internal secondary electron (SE) and movement toward surface can be simulated using this model. This model also takes into account the influences of incident angle and backscattering electrons as well as the surface gas contamination. In order to describe internal electronic states accurately, the penetration coefficient of incident electron is described as a function of material atom number. Directions of internal electrons are set to be uniform in each angle. The distribution of internal SEs is proposed by considering both the integration convergence and the cascade scattering process. In addition, according to the experiment data, relationship among desorption gas quantities, sample ultimate temperature and SEY is established. Comparing with experiment results, this synthetic semi-empirical physical model can describe the SEY of metal better than former formulas, especially in the aspect of surface contaminated states. The proposed synthetic semi-empirical physical model and presented results in this paper can be helpful for further studying SE emission, and offer an available method for estimating and taking advantage of SE emission accurately.

Keywords: secondary electron yield, synthetic semi-empirical physical model, metal, electron irradiation

PACS: 79.20.Ap, 72.20.Dp, 02.70.Uu, 72.80.Le **DOI:** 10.1088/1674-1056/26/9/097901

1. Introduction

Secondary electron (SE) has been investigated widely and used in many electronic fields since it was reported by Austin and Strake in 1902.[1] With detecting SEs due to the irradiation of focused electron beams, one can obtain surface images on a micro scale.[2] The SE multiplication between plates can conduce to magnifying the number of electrons.[3,4] Nevertheless, the generation of SEs may deteriorate the performance of device,[5] such as electron cloud due to high energy particle collision in accelerators, and multiplication effect of microwave device in the space environment.[6] For using or restraining SE emission better, it is important to calculate the yield of SE from material.[7] Furthermore, considering the fact that material used in device is contaminated more or less,[8] the investigation of secondary electron yield (SEY) in complicated surface states is still required.

The SEs are the electrons emitted from material surface, including true secondary electrons (TSEs) and backscattering secondary electrons (BSEs).[9] Those TSEs are generated by inelastic scattering events between incident electrons and material extra-nuclear electrons, while elastic scattering events between incident electrons and material nuclei may result in BSEs.[10] Yield of SE due to electron irradiation can be calculated with both Monte Carlo (MC) numerical simulations and formulas directly.[11] Since SEY is calculated by tracing each scattering events of electron inside the material in MC simulations, the computation of those simulations is always huge, and the accuracies of their results are limited. On the other hand, the yield of SEs can be quickly obtained with some classical formulas,[12] such as Joy, Vaughan and Furman's formulas.[13–16] Due to the simplification of direction and energy distributions of internal SEs and the ignorance of the contribution of backscattering SEs, Joy and Vaughan's formulas have an obvious deviation from experiment data in the case of high energy electron irradiation. And the experimental data fitted Furman formula requires assigning as many as twenty parameters for each material.[17] In addition, SEY of surface contaminated materials is still unclear in physics and needs further investigations.

In this paper, we propose a synthetic semi-empirical physical model of SEY of some ordinary metals, Ag, Al, and Au. This model performs processes of internal SEs excitation, outgoing toward surface, incident angle, and backscattering revises. Penetration coefficient of incident electron is corrected

*Project supported by the National Natural Science Foundation of China (Grant Nos. U1537211 and 11675278) and the China Postdoctoral Science Foundation (Grant No. 2016M602944XB).

†Corresponding author. E-mail: cuiwanzhao@163.com

© 2017 Chinese Physical Society and IOP Publishing Ltd

for the materials. Internal SEs are treated by using a more precise model. In addition, according to experimental data, we make a further investigation on one of important surface contaminations, i.e., surface gas adsorption. This research can help understand the influences of relevant parameters and surface states on SE emission, and has significance for application and restraint of SE in relevant fields.

2. Simulation method and results

Emission processes of SEs from a metal material are illustrated in Fig. 1, including internal SE excitation, outgoing of SEs from the inside, and SE emission across surface potential. In addition, SE emission is still related to incidence angle, backscattering, and surface contamination.

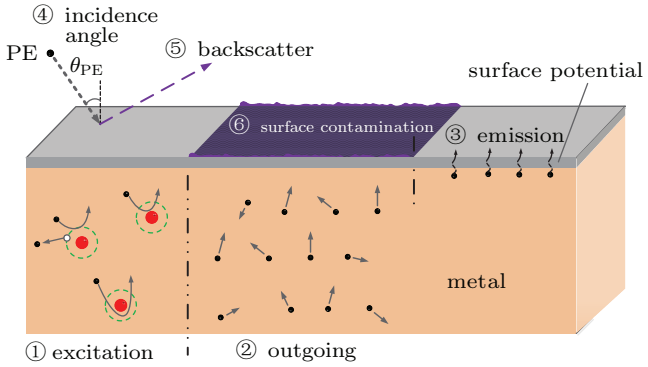


Fig. 1. (color online) Schematic of SE emission performed in this paper.

2.1. Excitation of internal secondary electron

Internal SE can be generated inside the material due to energetic electron beam irradiation. Primary electron with a larger kinetic energy can reach a deeper position, and the lateral range of the internal SE is also larger. For most amorphous materials, the range of internal SE $R(E_{pe})$ and the incidence electron energy E_{pe} are related by

$$R\left(E_{pe}\right)=\frac{L_k}{\rho_r}\left(\frac{E_{pe}}{E_k}\right)^{\alpha}, \tag{1}$$

where L_k is the Lane–Zaffarano constant and set to be 76 nm,[18] ρ_r is the relative material density, E_k is the standard energy (1 keV), and α is the index parameter and presents the capability of incident electron penetration. Lane and Zaffarano thought that α was a constant which was independent of materials, but the calculated results using the model under this presupposition cannot accord well with experimental results in the case of low-energy-electron incidence. Then, through analyzing NIST data and simulating electron scattering process with Monte Carlo method, we find the following rules.

1) A material with a higher atomic number has a larger deflection angle during the elastic scattering between incident electron and atom, and it will weaken the capability of incident electron penetration consequently.

2) A material with a higher atomic number has more orbital electrons and loses energy with a higher probability during the inelastic scattering between incident electrons and orbital electrons. It may also weaken the capability of incident electron penetration.

According to the quantitative analysis, we propose a relationship between parameter α and material atomic number (mainly for the metals: Al, Au, Ag, Cu, etc.) by

$$\alpha=1.26+0.46\exp\left(-Z/19.92\right). \tag{2}$$

As shown in Fig. 2(a), the parameter α decreases with atom number z increasing, which means that the material with a less atom number allows primary electrons to penetrate deeper.

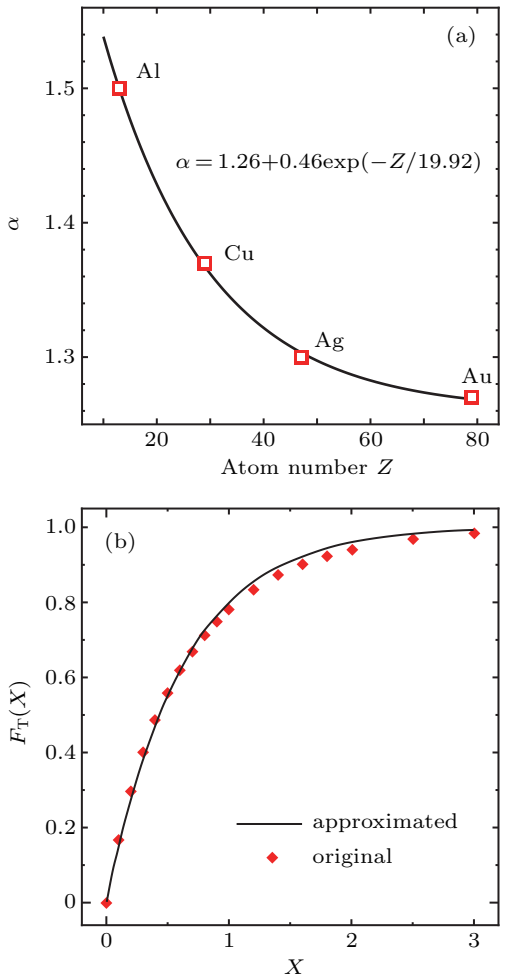


Fig. 2. (color online) (a) Parameter α as a function of material atom number Z; (b) comparison between Eq. (8) and its approximated function (9).

The internal SEs are excited inside the material due to inelastic scattering process after primary electron irradiation. Although distributions of internal electrons at different positions are different from each other, the internal SE distributions at SE emission related surface positions are almost the same. Hence, we can treat the distribution of internal SE in

deep $n(z)$ such that the following equality holds:

$$n(z) = \frac{N(E_{pe})}{R(E_{pe})}. \tag{3}$$

Here, $R(E_{pe})$ is the range of incident electron and $N(E_{pe})$ is the total number of internal SEs.

2.2. Outgoing from the inside

In the processes of elastic and inelastic scatterings, part of internal SEs can reach the surface of material and exit after crossing the surface potential barrier, while others deposit inside the material and trapped by defective atoms. Bruining[19] and Wittry[20] simplified the directions of internal SEs into upward and downward. Actually, directions of internal SEs can be arbitrary. Hence, we propose absorption probability $p_{abs}(ds)$ of internal SE at a distance ds in each direction can be expressed as

$$p_{abs}(ds) = \gamma ds. \tag{4}$$

Here, γ is the absorption coefficient and obeys the exponential distribution. An internal SE in the direction of φ at depth z passes through a distance of $z/\cos\varphi$ to reach material surface as shown in the following figure. Then, the probability with which an internal SE in the direction of φ at depth z can reach the material surface is

$$p(z,\varphi) = \exp\left(-\frac{z}{\lambda\cos\varphi}\right), \tag{5}$$

where λ is the mean free path of electron in material (for the ordinary metal Au, Ag, Cu, and Al, their values of λ are 1.6, 1.4, 1.2, and 3.8 nm, respectively).

Meanwhile, when an internal SE moves inside the material, it may crash with atom inelastically and generate another internal SE as well, which is cascade scattering. For amorphous material, this collision is isotropic, and directions of internal SEs after this process can be thought to be homogeneous. In general, the density of internal SEs at depth z is $n(z)$, we can obtain the number of internal SEs in the direction $\varphi \sim \varphi + d\varphi$ at the depth $z \sim z + dz$ which can reach the following material surface:

$$n(z,\varphi)\, p(z,\varphi)\, dz d\varphi = \frac{1}{2} n(z) \sin\varphi \exp\left(-\frac{z}{\lambda\cos\varphi}\right) dz d\varphi. \tag{6}$$

Combining the density of internal SEs with SE distribution at a depth, the total number of surface SEs N_s from the inside of material can be obtained from the following equation:

$$N_s = \int_0^{R(E_{pe})} n_s(z)\, dz = \frac{N(E_{pe})\,\lambda}{4R(E_{pe})} F_\Gamma\left(\frac{R(E_{pe})}{\lambda}\right). \tag{7}$$

Here,

$$F_\Gamma(x) = 2\int_0^x \left(\exp(-x') - z\Gamma(0,x')\right) dx', \tag{8}$$

which is acomplicated function and can be approximated as

$$F_\Gamma(x) \approx 1 - \exp(-1.6x). \tag{9}$$

Figure 2(b) shows the difference between the approximated functions (8) and (9). In Eq. (8), Γ is the gamma function $\Gamma(a,z) = \int_z^\infty t^{a-1} e^{-t} dt$. Then, the total number of surface SEs N_s is expressed as

$$N_s = \frac{N(E_{pe})\,\lambda}{4R(E_{pe})}\left(1 - \exp\left(-1.6\frac{R(E_{pe})}{\lambda}\right)\right). \tag{10}$$

Besides, we still have to figure out the energy distribution of internal SEs, which is related to the emission of internal SEs at the surface. Lin and Joy[13] thought that the internal SE energy equals the average ionization energy, while Streitwolf[21] set the energy distribution of internal SEs $S(E_s)$ as $S(E_s) \propto (E_s - E_F)^{-2}$. However, there is an essential problem under this assumption, the integration of all the internal SEs whose energy larger than E_F is not convergent. That means that the internal SEs could be innumerable, which conflict with realistic scenario obviously. In addition, this assumption only considers the internal SEs generated by incident electrons, and ignores the cascade scattering process.

Therefore, in this paper, we propose an energy distribution of internal SEs with taking into consideration both the integration convergence and the contribution from the cascade scattering process

$$S_R(E_s) = A\exp\left(-\frac{E_s - E_F}{E_v}\right). \tag{11}$$

Here, E_s is the energy of internal SE, E_v is the expected value of E_s, and E_F is the Fermi level of material. According to the law of energy conservation, the sum energy of all internal SEs should equal primary electron energy. Considering the fact that the energy of internal SEs is on the basis of Fermi level E_F, the sum energy of all internal SEs can expressed as

$$N(E_{pe}) \int_{E_F}^{E_{pe}} S_R(E_s)(E_s - E_F)\, dE_s = E_{pe}, \tag{12}$$

where $S_R(E_s)\, dE_s$ can represent the probability of internal SEs in an energy range of $E_s + dE_s$. The maximum of internal SEs is primary energy E_{pe}.

2.3. Emission from the surface

After reaching the surface, the internal SEs still need to cross the surface potential barrier before being emitted from the material surface, and its probability $p_e(E_s)$ mainly depends on barrier height U and internal SE energy E_s and is expressed as

$$p_e(E_s) = \begin{cases} 0, & E_s \le U, \\ \dfrac{4\sqrt{1 - U/E_s}}{\left(1 + \sqrt{1 - U/E_s}\right)^2}, & E_s > U, \end{cases} \tag{13}$$

and then based on the number of internal SEs, the SEY can be expressed as

$$\delta = N_s P_s = \frac{N(E_{pe}) P_s \lambda}{4R(E_{pe})} \left(1 - \exp\left(-1.6\frac{R(E_{pe})}{\lambda}\right)\right). \quad (14)$$

When the primary energy E_{pe} is much larger than Fermi level E_F, $N(E_{pe})$ can be approached as $N(E_{pe}) = E_{pe}/E_v$. Hence, we can obtain SEY

$$\delta = N_s P_s = \frac{E_{pe} P_s \lambda}{4E_v R(E_{pe})} \left(1 - \exp\left(-1.6\frac{R(E_{pe})}{\lambda}\right)\right). \quad (15)$$

The SEY is a function of primary energy $\delta(E_{pe})$. Primary electron with peak energy E_m generates a maximum SEY δ_m. Assuming its range $R_m = R'\lambda$, the equation above can be expressed with R'

$$1.6R' = \left(1 - \frac{1}{\alpha}\right)\left(\exp(1.6R') - 1\right). \quad (16)$$

As α is given by Eq. (2), the R' values of metals Al, Cu, Ag, and Au can be calculated to be 1.19, 1.39, 1.53, and 1.61, respectively. The peak energy E_m can be calculated from

$$E_m = E_k \left(\frac{R'\rho_r \lambda}{L_k}\right)^{1/\alpha}, \quad (17)$$

and the SEY can be expressed as

$$\delta = \frac{\delta_m}{1 - \exp(-1.6R')} \left(\frac{E_{pe}}{E_m}\right)^{1-\alpha} \times \left(1 - \exp\left(-1.6R'\left(\frac{E_{pe}}{E_m}\right)^{\alpha}\right)\right). \quad (18)$$

Here, maximum SEY δ_m satisfies

$$\delta_m = \frac{E_m P_s}{4E_v R'}\left(1 - \exp(-1.6R')\right). \quad (19)$$

2.4. Modification considering the incident angle

As many researches think that the SEY increases with incidence angle increasing, hence, in this paper, we should treat SEY semi-empirical physical model also with an incidence angle revision. When the incidence angle is θ, the depth range of primary electron can reach $R\cos\theta$, where R is the range in the case of vertical incidence. The distribution of internal SEs with incidence angle θ_{in} in should be revised as $n(z, \theta_{in}) = n(z)/\cos\theta$. Then, the number of internal SEs that can reach the surface in a depth $z \sim z + dz$ is

$$n_s(z)\,dz = \frac{N(E_{pe})}{2R(E_{pe})\cos\theta}\left(\exp\left(-\frac{z}{\lambda}\right) - z\Gamma\left(0, \frac{z}{\lambda}\right)\right)dz. \quad (20)$$

The upper limitation of integral of the total number of surface electrons $N_s(\theta)$ should be $R\cos\theta$. The peak energy of primary electron with incident angle θ_{in}, and its corresponding maximum SEY $\delta_m(\theta_{in})$ can be expressed respectively as

$$E_m(\theta_{in}) = \left(\frac{R'\rho\lambda_\theta}{B}\right)^{1/\alpha} = E_m(0)\left(\frac{1}{\cos\theta_{in}}\right)^{1/\alpha},$$

$$\delta_m(\theta_{in}) = \delta_m(0)\left(\frac{1}{\cos\theta_{in}}\right)^{1/\alpha}, \quad (21)$$

under the assumption of $\lambda_\theta = \lambda/\cos\theta_{in}$. The SEY of metal with primary electron irradiation at incident angle θ is

$$\delta(\theta) = \frac{\delta_m(\theta)}{1 - \exp(-1.6R')}\left(\frac{E_{pe}}{E_m(\theta)}\right)^{1-\alpha} \times \left(1 - \exp\left(-1.6R'\left(\frac{E_{pe}}{E_m(\theta)}\right)^{\alpha}\right)\right). \quad (22)$$

In the processes we performed above, trajectories of PEs are thought to be straight lines, which is reasonable when the incident angle is less than 60°. Hence, this incident angle revision of SEY is available within an angle range of 0–60°.

2.5. Modification with considering the electron backscattering

Apart from internal electrons which can escape from material surface, electrons due to backscattering of primary electrons can also emit from the surface, and constitute the total SEs. Those backscattering SEs include two parts, one is caused by the reflection surface potential barrier, while the elastic scattering between surface material atoms and primary electrons produces the other part. The reflection yield is

$$\eta_1(E_{pe}) = \eta_1(0)\exp\left(-\frac{E_{pe}}{E'_{BS}}\right). \quad (23)$$

Here, $\eta_1(0)$ is the backscattering coefficient of PEs with low energy. For an absolutely clean surface, it should be 0, while it is set to be 0.6 for a gas-adsorbed surface. The E'_{BS} is set to be 12.5 eV. Combining the elastic backscattering yield in the case of vertical incidence and the contribution from the effect of incident angle, we can obtain the following elastic scattering yield with the incident angle $\eta_2(E_{pe}, \theta)$:

$$\begin{aligned} &\eta_2(E_{pe}, \theta) \\ &= \eta_2(E_{pe}, 0)\left(1 + e_1(1 - \cos^{e_2}\theta)\right) \\ &= \eta_2(\infty)\left(1 - \exp\left(-\frac{E_{pe}}{E_{BS}}\right)\right)\left(1 + e_1(1 - \cos^{e_2}\theta)\right). \end{aligned} \quad (24)$$

Here, $\eta_2(\infty)$ elastic backscattering yield in high energy which is related with materials, and E_{BS} relative backscattering energy which is related with materials as well, e_1 and e_2 is backscattering revision parameters, which are set to be 0.8 and 0.4 for metals, respectively. Therefore, the total backscattering yield can be expressed as the sum of η_1 and η_2, $\eta_{BS} = \eta_1 + \eta_2$. Then, the total SEY can be revised as

$$\delta_{total} = \eta_{BS} + (1 - \eta_{BS})\,\delta. \quad (25)$$

2.6. Experiment comparison

For verifying the theory we performed above, we compare the theoretical results with experimental data of kinds of metals under electron beam irradiation. Since the ordinary metal surface is always contaminated due to oxidization and adsorption, we clean metal surface with Ar ion irradiation before testing their SE emission characteristics.

Figure 3(a) shows the measurement system of SEY. The vacuum environment of the main cavity can reach as high as 10^{-9} Pa. The electron gun works in a range of 20 eV–5000 eV, and its current is in a range between 0.05 nA and 2 nA. Samples are fixed on the platform which is rotatable and moveable in any direction. In addition, temperature of sample can be controlled by the heater under the stage. The default temperature of sample is ordinary room temperature 300 K.

Figure 3(b) shows the comparison of SEY curve of Ag between calculated results and experimental results. It is easy to find out that the simulation results calculated with this model accord with experimental results better than those with other models, such as Joy's and Vaughan's,[13,22] which can also verify the validity of our model.

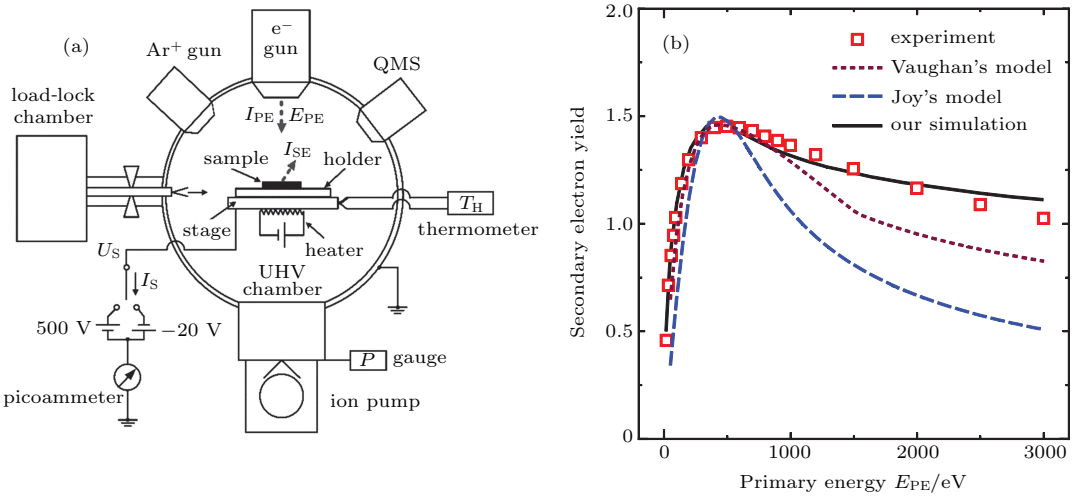
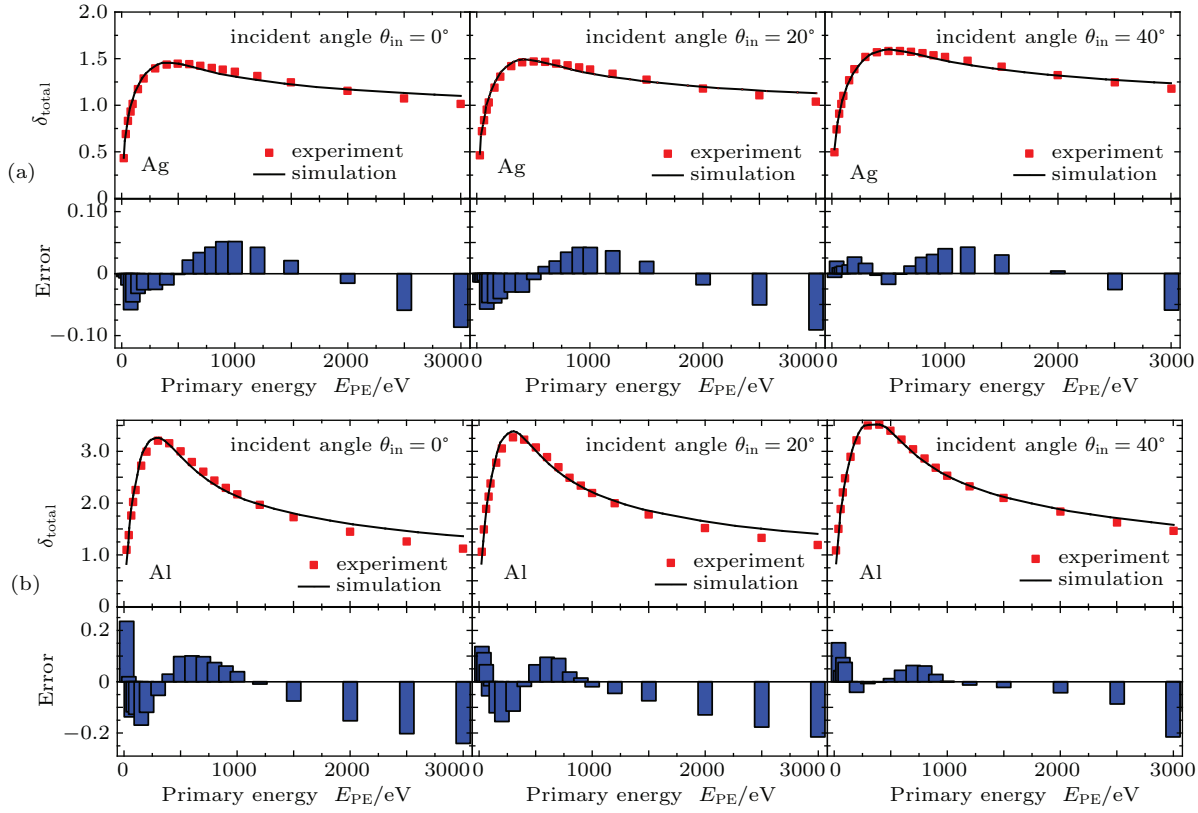


Fig. 3. (color online) (a) Schematic of SE measurement system; (b) comparation of SEY of the simulation with experimental data, by using the Joy and Vaughan's model.



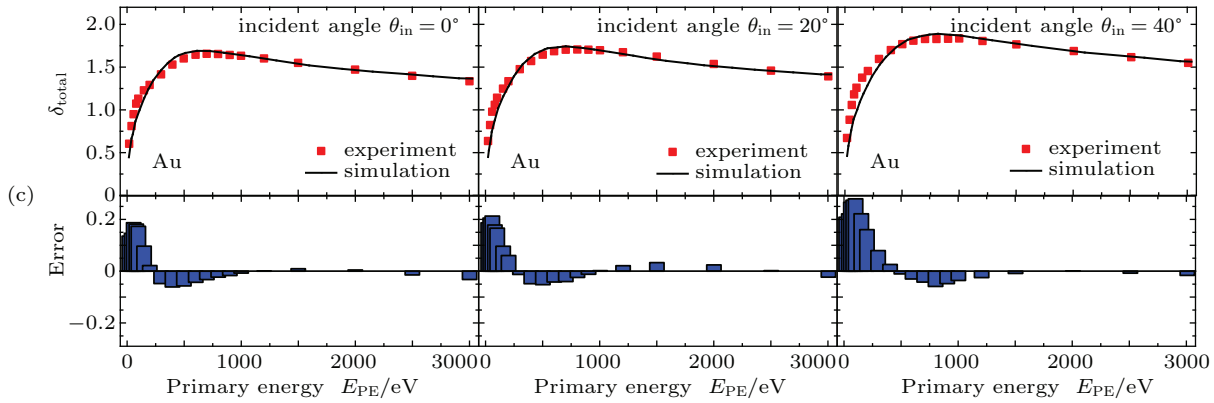


Fig. 4. (color online) Comparisons of SEY curve of (a) Ag, (b) Al, and (c) Au between calculation and experiment results at angles of 0°, 20°, and 40°.

Table 1. Parameters setting of SEY related metals.

Metals	U/eV	α	R'	E_m/eV	δ_m	$\eta_2(\infty)$	E_{BS}/eV
Ag	4.53	1.3	1.5	391	2.06	0.55	29.1
Al	2.56	1.57	1.11	281	5.28	0.46	46.1
Au	5.1	1.27	1.61	731	2.36	0.56	23.9

Table 1 is SEY related parameters setting of metals (Ag, Al, and Au), which are corresponding with Fig. 4. Figure 4 includes the total SEY δ_{total}, errors of SEY test under different primary electron energy irradiations. Results of calculations for metals approximately accord with experimental data.

In addition, the comparisons shown in Fig. 4 still include SEY and their errors at different incident angles for three metals, Ag, Al, and Au. The agreement between experimental results and simulation results can also indicate the applicability of our model in incident angle revision. On the whole, comparison differences in Ag between experimental results and simulation results metals are not so notable as those in Au and Al.Error comparison results also show that this model produces more consistent results with experimental data when the incident energy is larger.

2.7. Surface contamination

For metals in the ordinary environment in air, their characteristics of SE emission is also related to surface contamination state. Generally, surface contaminations contain adsorbed gases and oxide layers for most parts. On the one hand, those contaminations may reduce the escape depth of internal SEs, and thus change the peak energy E_m. On the other hand, contaminations may also change the surface potential barrier U and the mean energy of internal SEs E_v, then affect the process of SE emission.

Table 2 shows the values of mean free path λ of four metals (Au, Ag, Cu, and Al) exposed to the air environment for a long time. We can find that λ values of those metals in air environment are lower than those with a clean surface state. Then, based on Eq. (17), the peak energy E_m can be obtained.

Table 2. Mean free paths of metals exposed to air environment.

Materials	Atom number Z	Mean free path λ/nm
Au	79	1.4
Ag	47	0.7
Cu	29	0.9
Al	13	3.7

Considering the fact that the quantity of surface adsorbed gas is hard to modify directly in experiment, we describe the quantity of surface adsorbed gas with metals heated to some certain temperatures in this research. Taking Ag for example, we try to figure out the relationship between the ultimate temperature and the desorption gas quantity. By heating five silver samples with the same initial states to different ultimate temperature T_S, we obtain changes of surface adsorbed gas quantity Q_S of each silver sample. Those heating and testing processes are finished in vacuum environment with the SE measurement system as we mentioned above.

Figure 5 shows the desorption gas quantity Q_S as a function of ultimate sample temperature T_S. The relationship between Q_S and T_S can be expressed as

$$Q_S = 1.6\exp(T_S/177.2) - 2.8. \tag{26}$$

After adsorbed gas is released from the surface, the work function of the surface may change, and SEY varies consequently. Since the work function of metal after being heated in vacuum is hard to measure in experiment, we can adapt the work function for the measured SEY, and obtain the maximum SEY δ_m and function of work function U as a function of ultimate sample temperature T_S and desorption gas quantity Q_S as shown in Fig. 6.

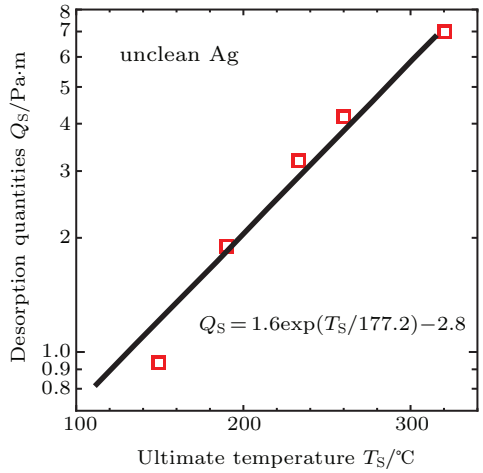


Fig. 5. (color online) Desorption gas quantity Q_S as a function of ultimate sample temperature T_S.

As shown in Fig. 6(a), we can find that the maximum SEY δ_m decreases linearly with ultimate sample temperature T_S, while the work function U increases exponentially in the range shown in the figure. And a similar relationship of the desorption gas quantity Q_S is shown in Fig. 6(b), which can be fit with an exponential function

$$U(\text{eV}) = 3.34 + 0.11\exp(Q_S(\text{Pa}\cdot\text{m})/0.29). \quad (27)$$

Considering the relationship between ultimate temperature T_S and desorption gas quantities Q_S, the maximum SEY δ_m can be expressed by the ultimate temperature T_S as

$$\delta_m = 3.548 - 0.00355T_S. \quad (28)$$

Then, with the revision of surface contamination on SEY, we compare SEY calculation results of unclean silver at three different temperatures $T_S = 108$ °C, 233 °C, 320 °C with experiment results as shown in Fig. 7.

Since the silver easily adsorbs gas in air environment, gases will escape from the surface after heat processing, and then the work function increases and the SEY reduces as a consequence. As shown in the figures above, calculated results accord well with experimental data after revising the work function and mean free path in the case of surface contamination.

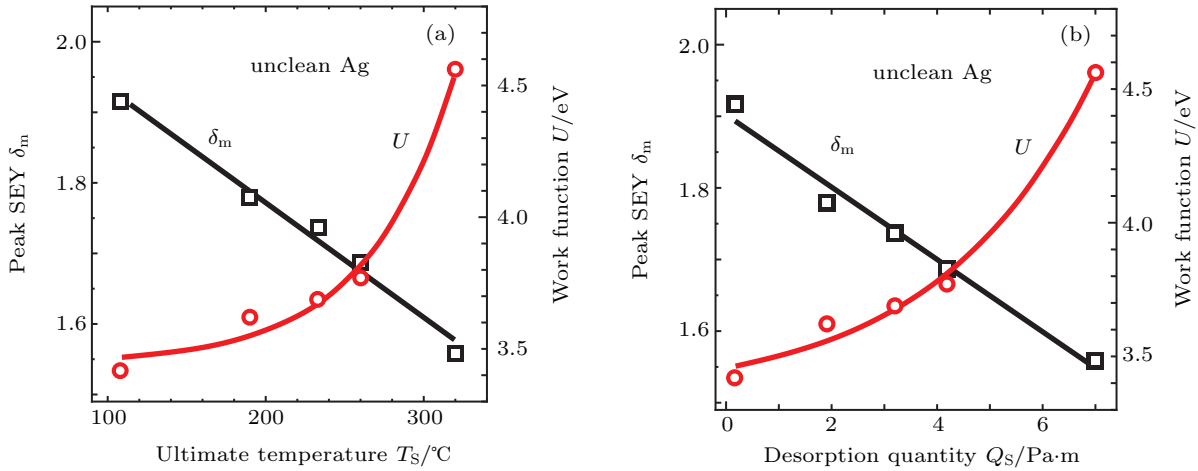


Fig. 6. (color online) Variations of maximum SEY δ_m and work function U with (a)ultimate sample temperature T_S and (b) desorption gas quantity Q_S for unclear Ag.

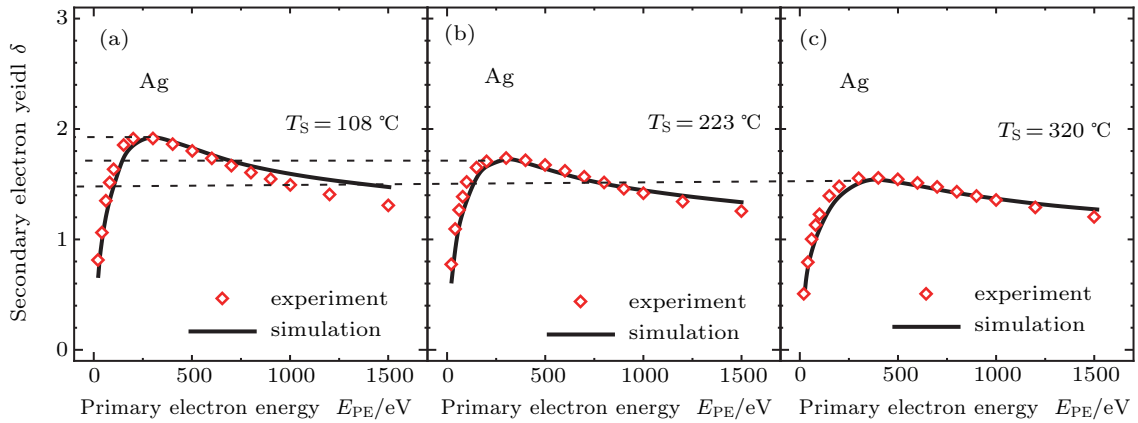


Fig. 7. (color online) Comparison of δ varying with E_{PE} between calculations and measurements of uncleaned silver at three different ultimate temperatures $T_S = 108$ °C (a), 233 °C (b), 320 °C (c).

3. Discussion

The results obtained from the presented synthetic semi-empirical physical model of SEY accord with experimental results better than those from the model proposed by Joy and Vaughan. By revising the penetration parameter α for different materials with the NIST database, the range of internal SE distribution can be presented more accurately than the case that the penetrated parameter is set to be the same constant. In addition, compared with the method of the former model, the method of this model sets the directions of internal SEs to be isotropic and treats the internal SEs energy with a convergent distribution, which correspond to a precise SEY.

For a sample exposed to air for a long time, the surface contaminations of metal material should include adsorbed gas and oxides in general. In this paper, effects of surface absorbed gas on SEY are investigated as a primary factor. Actually, for some active metals, oxidization of surface layer also has a remarkable effect on SE emission, which still needs further investigations.

4. Conclusions

In this paper, we propose a synthetic semi-empirical physical model for SEY of metals. With expressing the penetrated parameter as a function of atom number, revising the direction and energy distribution of internal SEs, and considering the contribution of backscattering electron, the formula for SEY in this article performs much better than the previous one in the sense of its agreement with experimental results. In addition, a relationship between work function and adsorbed gas quantity is established in the way of heating sample. The effects of temperature on SEY are expressed with a formula directly. Results show that the desorption gas quantity increases with ultimate sample temperature increasing exponentially, and surface work function increases with desorption gas quantity increasing exponentially as well. Then, the maximum SEY presents a linear increase relationship with ultimate sample temperature increasing, as a consequence. This work can conduce to understanding the emission of SE from metal surface, and has a significance for studying the surface contamination effects.

References

[1] Austin L and Starke H 1902 *Annalen. Der. Physik.* **314** 271
[2] Al-Obaidi H N and KhaleelI H 2013 *Micron* **51** 13
[3] Feng G B, Cao M, Yan L P and Zhang H B 2013 *Micron* **52–53** 62
[4] Feng G B, Wang F, Hu T C and Cao M 2015 *Chin. Phys. B* **24** 117901
[5] Wang F, Feng G B, Zhang X S and Cao M 2016 *Micron* **90** 64
[6] He Y N, Ye M, Hu S G 2013 *J. Appl. Phys.* **113** 074904
[7] Weng M, Cao M, Zhao H J and Zhang H B 2014 *Rev. Sci. Instru.* **85** 036108
[8] Zhang H B, Hu X C, Wang R, Cao M, Zhang N and Cui W Z 2012 *Rev. Sci. Instru.* **83** 066105
[9] Suzuki M, Kumagai K, Sekiguchi T, Cassell A M, Saito T and Yang C Y 2008 *J. Appl. Phys.* **104** 114306
[10] Feng G B, Wang F and Cao M 2015 *Acta Phys. Sin.* **64** 227901 (in Chinese)
[11] Renoud R, Mady F, Bigarre J and Ganachaud J P 2005 *J. Euro. Cera. Soci.* **25** 2805
[12] Bundaleski N, Shaw B J, Silva A G, Moutinho A M C and Teodoro O M N D 2011 *Scanning* **33** 266
[13] Lin Y and Joy D C 2005 *Surf. Interf. Anal.* **37** 895
[14] Furman M A and Pivi M T F 2013 *Phys. Rev. Accel. Beams* **16** 069901
[15] Vaughan J R M and Abuelma'Atti M T 1991 *IEEE Trans. Electron. Dev.* **38** 1982
[16] Vaughan J R M 1989 *IEEE Trans. Elec. Devi.* **36** 1963
[17] Furman M A and Pivi M T F 2002 *Phys. Rev. St. Accel. Beams* **5** 124404
[18] Lane R O and Zaffarano D J 1954 *Phys. Rev.* **94** 960
[19] Bruining H 1955 *Physics and Applications of Secondary Electron Emission* (London: Pergamon Press) pp: 93–96
[20] Wittry D B and Kyser D F 1965 *J. Appl. Phys.* **36** 1387
[21] Streitwolf H W 1959 *Annalen. Der. Physik.* **458** 183
[22] Vaughan R 1993 *IEEE Trans. Electron. Dev.* **40** 830